International Journal of Thin Films Science and Technology

http://dx.doi.org/10.18576/ijtfst/110104

Improved Physical Properties of ZnO Films with a second Superposed SnO2 very Thin Films Deposited by Spray Pyrolysis Method

K. Salim[*] *and M. N. Amroun*

Materials Development and Characterization Laboratory, Department of Electronics, Djillali Liabes University, BP89, Sidi Bel Abbés 22000, Algeria

Received: 21 Jul. 2021, Revised: 12 Aug. 2021, Accepted: 13 Oct. 2021.
Published online: 1 Jan. 2022.

Abstract: ZnO Thin films were deposited on glass substrates at 350 ± 10 0C by pyrolysis spray technique. A very thin layer of SnO2 was deposited under ZnO films for the purpose of getting a bilayer thin SnO2/ ZnO. A thermal annealing was carried out for the bilayer with a temperature of 350 0C for one hour. The structural, optical and electrical properties of monolayer ZnO films and SnO2/ZnO bilayer thin films were investigated. X-ray diffraction confirmed the hexagonal wurtzite structure of ZnO films, and the hexagonal tetragonal structure of SnO2/ZnO bilayer films. The optical measurement showed a rise of the average transmittance from 81 % to 94 % for SnO2/ZnO annealed bilayer films. The optical band gap varied between 3.22 to 3.31 eV for SnO2/ZnO annealed bilayer films. The maximum electrical conductivity of 17.85 (Ω .cm-1) has been observed for SnO2/ZnO annealed bilayer films.
Keywords: Thin film, zinc oxide, spray pyrolysis, band gap.

1 Introduction

Transparent conductive oxides (TCO) are currently of great commercial and scientific importance and are widely used in applications in electro-optical devices [1], gas sensors [2] and solar cells [3], because to the high transmittance in the ultraviolet visible (UV - Vis) range wavelength and electrical conductivity [4,5]. The TCO/Metal and TCO/TCO structure have been manufactured to enhance the TCO properties towards solar photovoltaic applications [6,7,8].

In recent years, zinc oxide (ZnO) has been of increasing interest in many research works because of its many potential applications. ZnO is a nontoxic (II-VI) binary semiconductor material [9] with very interesting characteristics such as piezoelectricity [10], photoconductivity [11], optical waveguides [12], gas probes [13], excellent electrical, optical, mechanical, and chemical sensing properties, as well as thermal stability. These materials are wide-band-gap (3.27 eV) semi-conductors with a large (60 meV) exciton binding energy [14]. ZnO thin films can be obtained by several techniques such as pulsed laser deposition [15], thermal evaporation [16], sputtering [17], sol gel [18] and spray pyrolysis [19,20,21,22,23]. Several researchers have reported TCO characteristics of bilayer films involving ZnO and SnO_2 films such as Vaezi et al. [24], Ravikumar et al [25] and Anandhi et al [26].

Enhancement physical properties of the ZnO films by second superposed SnO_2 thin films and the thermal annealing of the SnO_2/ZnO bilayer are studied in this work. To the best of our knowledge, the enhancements of the properties of SnO_2/ZnO bilayer grown by spray pyrolysis technique have not yet been reported in the literature.

2 Experimental Details

2.1 Preparation of Thin films

The ZnO, SnO_2 and SnO_2/ZnO thin films were prepared on glass substrates using the spray pyrolysis technique as shown in fig.1. The glass substrates were cleaned by diluted hydrochloric acid (HCl) and acetone, washed by double distilled water and dried. The sprayed solutions have been obtained by dissolving zinc nitrate ($Zn(NO_3)_2$) (50ml) and tin chloride ($SnCl_2$) (20 ml), in doubly distilled water with a

[*]Corresponding author E-mail: karim22000@hotmail.com

concentration of (0.1 M), respectively; were used as host precursors.

In the samples preparation process, the following conditions have been considered: substrate temperature 350 ± 10 °C, solution flow of 2 ml /min and spray nozzle to heating plaque distance of 30 cm. We took two minutes interval time between spraying periods in order to avoid excessive cooling of the glass substrates resulting from continuous spray. One also noted that the prepared solutions were immediately sprayed to avoid any possible chemical changes with time. The structural characterization was performed at room temperature using a Bruker X-ray diffractometer model D2 Phaser with CuKα radiation (λ=1.5406 Å). The optical transmittances have been recorded between 200 and 2500 nm wavelength using a JASCO 570 type UV-visible-NIR double-beam spectrophotometer. The electrical parameters were measured by using the ECOPIA HMS-5000 Hall Effect measurement system at room temperature.

3 Results and Discussions

3.1 Structural Parameters

The XRD patterns of ZnO, SnO_2, SnO_2/ZnO and SnO_2/ZnO annealed bilayer films are shown in Fig. 2. The XRD patterns clearly show five well defined peaks for ZnO (100), (002), (101), (102) and (103) and three peaks for SnO_2 (110), (200) and (211). The SnO_2/ZnO bilayer thin films exhibited a The XRD patterns of ZnO, SnO_2, SnO_2/ZnO and SnO_2/ZnO annealed bilayer films are shown in Fig. 2. The XRD patterns clearly show five well defined peaks for ZnO (100), (002), (101), (102) and (103) and three peaks for SnO_2 (110), (200) and (211). The SnO_2/ZnO bilayer thin films exhibited a presence of the two phase of hexagonal wurtzite structure of ZnO (JCPDS N◦: 36-1451) [27,28] and the tetragonal structure of SnO_2 (JCPDS N◦: 041-1445) [29].

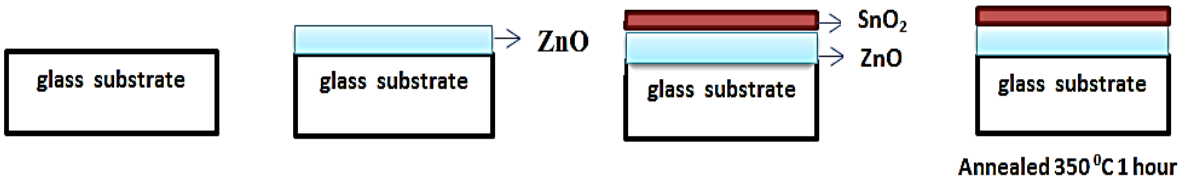

Fig.1: Sample models for ZnO, SnO_2/ZnO bilayer, and SnO_2/ZnO bilayer annealed films.

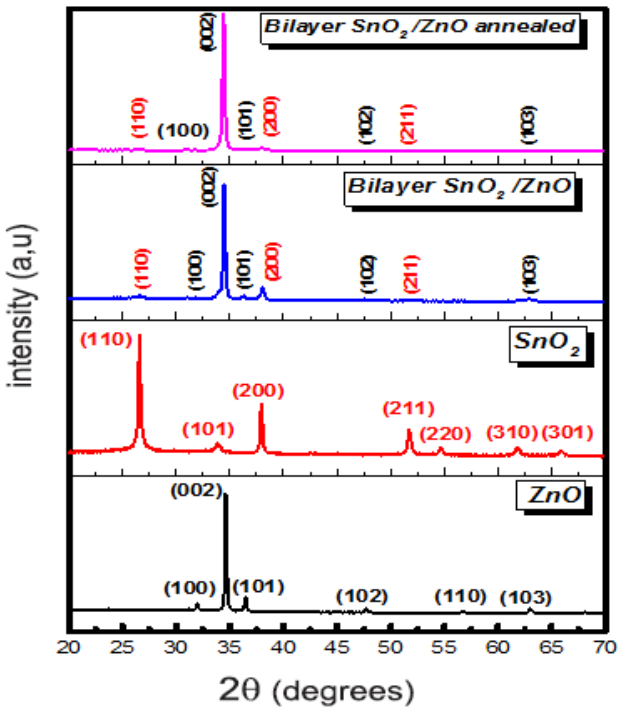

Fig.2: XRD patterns of ZnO, SnO2, SnO2/ ZnO Bilayer and SnO2/ ZnO Bilayer annealed films.

tetragonal structure were determined from XRD results using the following equation [28,29,30]:

$$\frac{1}{d_{hkl}^2} = \frac{4}{3}\left(\frac{h^2+hk+k^2}{a^2}\right) + \frac{l^2}{c^2} \quad (1)$$

$$\frac{1}{d_{hkl}^2} = \left(\frac{h^2+k^2}{a^2}\right) + \frac{l^2}{c^2} \quad (2)$$

Where: d is interplanar spacing, (hkl) are the miller indices. The lattice constant (a, c) and values are tabulated in (Table 1).

The calculated values ‘a’ and ‘c’ of all the films are in good agreement with those provided by the standard card of ZnO hexagonal phase (JCPDS N◦: 36-1451) with lattice parameters a=3.249A° and c=5.20 A°) and of SnO_2 tetragonal phase (JCPDS No. 41-1445) with lattice parameters a=4.738 A° and c=3.187 A°). A slight deviation has been observed from the bulk lattice parameters indicate the presence of stress/strain in the films, which might be caused by the defects, stoichiometric deviations and/or mismatch of thermal expansion coefficients of both the substrate and film [31].

The crystallite size (D) was calculated for preferential orientations using Scherer’s equation. In addition, structural defects such as micro-strain (ε) and

dislocation density (δ) were calculated using the following relations [32]: The calculated crystalline parameters of the films are regrouped in (Table 1)**.**

$$D = (0.9.\lambda)/(\beta.\cos\theta) \quad (3)$$

$$\varepsilon = \frac{\beta.\cos\theta}{4} \quad (4)$$

$$\delta = \frac{1}{D^2} \quad (5)$$

The crystallite size decreased from 34.67 nm for pure ZnO to 25.03 nm for bilayer SnO_2/ZnO, which can be attributed to increasing structural defects [33].

The crystallite size of bilayer films increased with annealing temperature from 25.03 nm to 26.597 nm, which can be attributed to activate atom diffusion and hence, facilitate to repairing the dislocated atomic occupancies and even promote the coalescence of adjacent particles [34-35]. The bilayer annealed films exhibited a less structural disorder (strain and dislocation density), which indicate improvement in the crystallinity of the films.

3.2 Optical parameters

The optical transmittance spectrum as a function of the wavelength for ZnO, SnO_2, the bilayer SnO_2/ZnO and SnO_2/ZnO annealed films deposited on glass substrates is showed in Figure 3. The SnO2/ZnO bilayer are highly transparent with an average transmission of 78-85% in the visible-IR region. The transmittance achieved 94 % for the bilayer films after annealing, which is requested for satisfactory optical window in visible range in photovoltaic systems [36]. Improving in the transmittance of the films could be explained by the reduction of surface roughness [36], to a low scattering effects resulting from the structural homogeneity of the films [39]. The deficiency of interference fringes in transmission spectra is due the surface roughness caused by the spray pyrolysis technique. This is maybe due to very small droplets resulting from this technique that vaporize above the glass substrates and condense as clusters [37]. The formula used to calculate the optical band gap energy of the films is [38]:

$$(\alpha h\nu)^n = A(h\nu - Eg) \quad (6)$$

Where α: Absorption coefficient; $h\nu$: Photon energy, A: relation constant, E_g: optical band gap. For: n=2 direct band gap semiconductors and n=0.5 indirect band gap semiconductors. The absorption coefficient α is derived from transmittance T using the beer-lambert law [28]:

$$\alpha = \frac{1}{t}\ln\frac{1}{T} \quad (7)$$

Where t: is the film thickness.

Table 1: Structural parameters of the deposited films.

Films	grain size D (nm)	a (A^0)	c(A^0)	ε Strain $.10^{-4}$	Density dislocation $.10^{-4}$ Line/nm^2
ZnO	34.670	3.240	5.183	09.991	08.319
SnO_2	28.300	4.720	3.186	11.701	12.486
Bi-layer SnO_2/ZnO	25.030	3.242	5.189	13.871	16.015
Bi-layer SnO_2/ZnO with annealing	26.597	3.241	5.186	13.039	14.141

Table 2: Optical parameters of the deposited films.

samples	Eg (eV)	Eu (eV)
ZnO	3.22	0.081
SnO_2	3.91	0.326
Bilayer SnO_2/ZnO	3.28	0.155
Bilayer SnO_2/ZnO annealed	3.31	0.142

The obtained optical band gap of the ZnO films is 3.22 eV and 3.91 eV for the SnO_2 films, which agrees with the literature [40]. The optical band gap increases from 3.22 eV for pure ZnO films to 3.28 eV SnO_2/ ZnO Bilayer. This gap blue shifting could be explained by the contribution of the Moss–Burstein effect of the degenerate energy levels are created with band filler which make the level of Fermi moves over the edge of the conduction band [41,42,43]. The optical band gap increases after annealed to 3.31 eV due to the oxygen diffusion with annealing temperature [44].

The disorder measure is characterized by Urbach tail. The Urbach energy is estimated from the variation of the absorption coefficient. This absorption coefficient of the films shows a tail for the photon energy sub-band [38]:

$$\alpha = \alpha_0 \exp\left(\frac{h\nu}{E_U}\right) \quad (8)$$

where α_0 is a constant and *Eu*: is the Urbach energy.The Urbach energy is found to increase from 0.081 eV for pure ZnO films to 0.155 eV of the SnO_2/ZnO bilayer (Table 2), due to an increase in structural disorder. This is consistent with the results from XRD analysis. The Urbach energy decreased from 0.155 for SnO_2/ZnO bilayer to 0.142 eV with annealing, which indicate the decrease in the structural disorder [44].

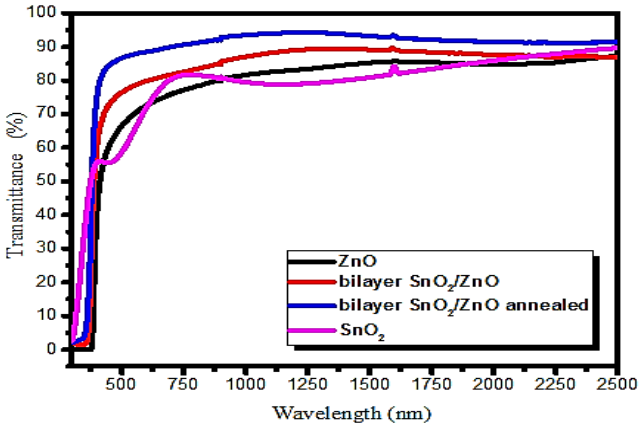

Fig. 3: Optical transmittance of the prepared films.

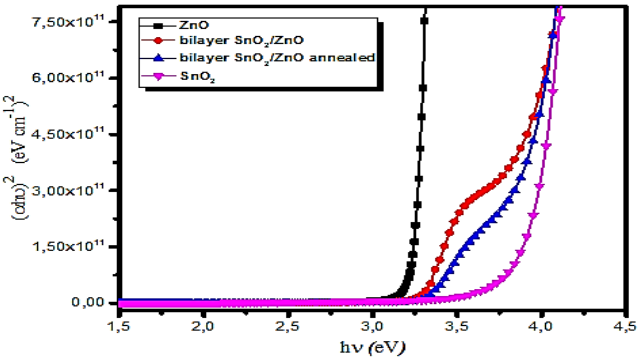

Fig. 4: Optical gap of ZnO, SnO_2, SnO_2/ ZnO Bilayer and SnO_2/ ZnO Bilayer annealed films versus $(\alpha h\nu)^2$.

3.3 Electrical Parameters

The electrical properties were measured by measuring ECOPIA HMS-5000 Hall Effect measurement system at room temperature. The negative values of carrier concentrations showed that as deposited films are n-type conductivity. It observed from Figure 5 that the conductivity of the films rises from 3.37 $\times 10^{-03}$ $(\Omega\ .cm)^{-1}$ for ZnO films to 17.85 $(\Omega\ .cm)^{-1}$ for SnO_2/ZnO bilayer annealed films. The increase in the electrical conductivity of the films could be assigned to increase in the carrier concentrations of the films from $3.66\times10^{+16}$ for pure ZnO films to $2.28.10^{+20}$ (cm^{-3}) for SnO_2/ZnO bilayer annealed films.

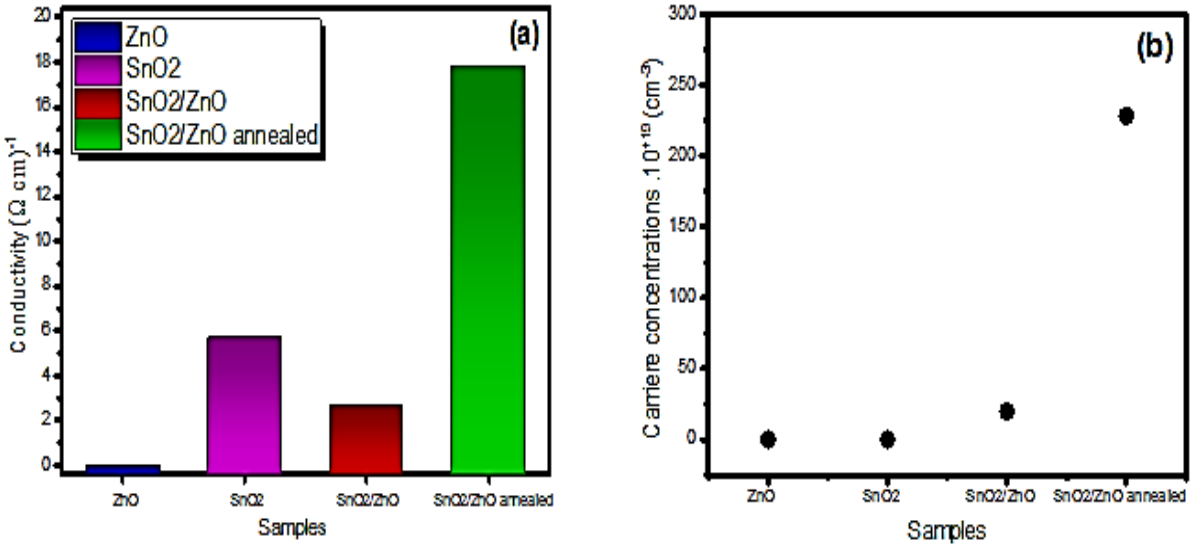

Fig. 5: (a) conductivity and (b) Carrier Concentrations of ZnO, SnO_2, SnO_2/ ZnO Bilayer and SnO_2/ ZnO Bilayer annealed films and SnO_2/ ZnO Bilayer annealed films.

Table 3: Electrical parameters of the deposited films.

Samples	Sheet Resistance (Rsh) (Ω/sq)	Mobilite (cm^2/Vs)	Carrier Concentrations (cm^{-3})	Conductivity (Ω.cm)
ZnO	1.01×10^{07}	5.78×10^{-01}	$-3.66\times10^{+16}$	$3.37.10^{-03}$
SnO_2	5.93×10^{03}	5.61×10^{-01}	$-6.33\times10^{+19}$	5.69
Bilayer SnO_2/ZnO	1.36×10^{04}	8.68×10^{-01}	$-1.89\times10^{+19}$	2.63
Bilayer SnO_2/ZnO annealed	2.01×10^{03}	4.59×10^{-01}	$-2.28\times10^{+20}$	17.85

3.4 Optical Electrical Performance

The good TCO material should exhibit a low resistivity and a good transmittance spectral at the same time. For that, we applied the same idea of Ref. [45] and constructed a 2D diagram composed of two contradictory TCO characteristics: the sheet resistance R_{sh} and the optical loss defined as 1-(at 400-800 nm). For an optimal comparison, we calculated (1-T) and R_{sh} for our SnO_2/ZnO annealed films (Figure 6). We also included other experimental values from 16 different references; SnO_2/ZnO annealed surpassed all our samples in terms of optical loss. From the figure 6, our sample SnO_2/ZnO annealed dominates the 16 experimental works in terms of optical loss and 9 in terms of sheet resistance. The subset, i.e. Refs [33,47] constitute the so called "Pareto front" or "Pareto set", it contains points that aren't dominated by the other points. Our greatest sample (SnO_2/ZnO bilayer annealed films) belongs to the present sub-optimal set.

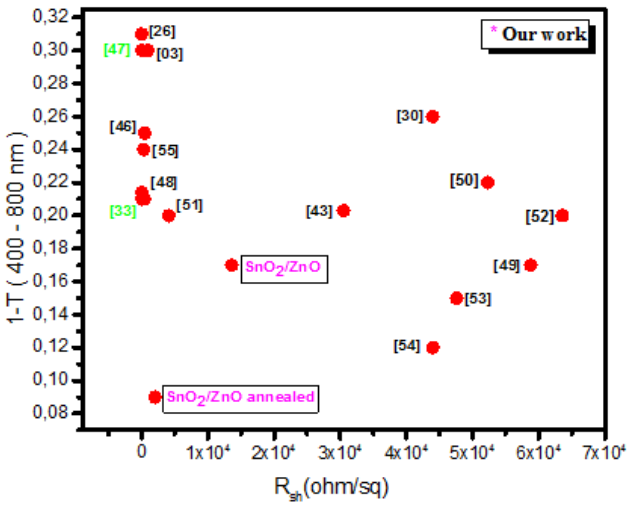

Fig. 6: A pareto front of SnO_2/ZnO and SnO_2/ZnO annealed thin films prepared in this work and literature.

4 Conclusions

In this study, good quality of SnO_2/ZnO bilayer grown by spray pyrolysis technique spray technique. The XRD profiles; the bilayer films have several peaks associated of the picks ZnO and SnO_2 films. The optical and electrical structural characterization demonstrate that the annealed bilayer films show good optical and electrical parameters, such as high transmittance in the visible range > 90 %, wide optical gap (Eg=3.31 eV), and high electrical conductivity (17.85 Ω.cm), asserting it is potential window layer for obtaining a high efficient solar cell.

References

[1] C.M. Muiva ,T.S. Sathiaraj, K. Maabong. Effect of doping concentration on the properties of aluminium doped zinc oxide thin films prepared by spray pyrolysis for transparent electrode applications, *Ceramics International*, **37**, 555-560(2011).

[2] M. Hjiri, L. El Mir, S.G. Leonardi, A. Pistone, L. Mavilia, G. Neri, Al-doped ZnO for highly sensitive CO gas sensors, *Sensors and Actuators B*, **196**, 413-420(2014).

[3] H. Çolak , E. Karakose. Tm-doped ZnO nanorods as a TCO for PV applications, *Journal of Rare Earths*., **36**, 1-7(2018).

[4] S. Benramache, A. Rahal, B. Benhaoua. The effects of solvent nature on spray-deposited ZnO thin filmprepared from Zn(CH3COO)2.2H2O, *Optik*, **125**, 663- 666(2014).

[5] N. Chahmat, T.Souier, A. Mokri, M. Bououdina, M.S. Aida, M. Ghers. Structure, Microstructure and Optical Properties of Sn-doped ZnO Thin Films, *Journal of Alloys and Compounds,* **593**, 148-153(2014).

[6] S.Calnan, A.N. Tiwari, High mobility transparent conducting oxides for thin film solar cells, *Thin Solid Films*, **518**, 1839-1849(2010).

[7] N. Chantarat, S. Hsu, C. Lin, M. Chiang, S. Chen. Mechanism of an AZO-coated FTO film in improving

the hydrogen plasma durability of transparent conducting oxide thin films for amorphous-silicon based tandem solar cells, *Journal of Materials Chemistry*, **22**, 8005-8012(2012).

[8] T. Fujibayashi, T. Matsui, M. Kondo, Improvement in quantum efficiency of thin film Si solar cells due to the suppression of optical reflectance at transparent conducting oxide/Si interface by TiO2 ZnO antireflection coating, *Applied Physics Letters*,**88**, (2006).

[9] A. Ouhaibi, M. Ghamnia, M.A. Dahamni, V. Heresanu, C. Fauquet, D. Tonneau. The effect of strontium doping on structural and morphological properties of ZnO nanofilms synthesized by ultrasonic spray pyrolysis method, *Journal of Science: Advanced Materials and Devices*, **3**, 29-36, 2018.

[10] L.Kang, H.An, J.Park, M.Hong, S.Nahm,C.Lee , *Applied Surface Science* , **475**,969-973 (2019).

[11] M. Farooqi, R. Srivastava. Structural, optical and photoconductivity study of ZnO nanoparticles synthesized by annealing of ZnS nanoparticles, *Journal of Alloys and Compounds*, **691**, 275-286 (2017).

[12] R. Fan, F. Lu, K. Li, Single-mode channel waveguide at 1540 nm in Er-doped ZnO thin film, *Journal of Luminescence*, **192**, 410-413(2017).

[13] T. Tesfamichael, C. Cetinb, C. Piloto , M. Arita, J. Bell, The effect of pressure and W-doping on the properties of ZnO thin films for NO2 gas sensing, *Applied Surface Science*, **357**, 728-734(2015).

[14] N. K. Hassan, M.R. Hashim, Structural and Optical properties of ZnO thin film prepared by Oxidation of Zn metal powders, *International Conference on Enabling Science and Tcehnology*, Johor Bahru, Malaysia, (2012).

[15] Y. Yolanda, D. Liu, P. Cheng, Pulsed laser deposition of zinc oxide, Thin Solid Films, **501**, 366-369 (2006).

[16] S. Navale, I.S. Mulla, Photoluminescence and gas sensing study of nanostructured pure and Sn doped ZnO, *Materials Science and Engineering C*, **29**, 1317-1320(2009).

[17] T.L. Yang, D.H. Zhang, J. Ma, H.L. Ma, Y. Chen, Transparent conducting ZnO:Al films deposited on organic substrates deposited by r.f. magnetron-sputtering, *Thin Solid Films*, **326**, 60-62(1998).

[18] S. Ilican, Y. Özdemir, M. Caglar, Y. Caglar, Temperature dependence of the optical band gap of sol-gelderived Fe-doped ZnO films, *Optik*, **127**, 8554-8561(2016).

[19] K. Salim , W. Azzaoui , M. N. Amroun, A.H. Kacha, Effect of Mn Doped and Mn+Sn Co-doping on the Properties of ZnO Thin Films, *International Journal of Thin Films Science and Technology*, **10**, 233-237 (2021).

[20] K. Salim, W. Azzaoui, M.N. Amroun , Influence of Doping Concentration on the Properties of Tin Doped Zinc Oxide Thin Films Prepared by Spray Pyrolysis for Photovoltaic Applications, *International Journal of Thin Films Science and Technology*,**10**,197-204(2021).

[21] M.N.Amroun, K. Salim, A.H.Kacha, Molarities Effect on Structural Optical and Electrical Properties of Nanostructured Zinc Oxide deposited by Spray Pyrolysis Technique, *International Journal of Thin Films Science and Technology*, **10**, 67-73(2021).

[22] M.N. Amroun, K. Salim, A.H.Kacha, M.Khadraoui. Effect of TM (TM= Sn, Mn, Al) Doping on the Physical Properties of ZnO Thin Films Grown by Spray Pyrolysis Technique: A comparative Study, *International Journal of Thin Films Science and Technology*, **9**, 7-19(2020).

[23] M.N. Amroun, K. Salim, A.H. Kacha, M. Khadraoui, H. Nguyen, H. Jeon, T. Kang. Fabrication of aluminium doped zinc oxide (AZO) transparent conductive oxide by ultrasonic spray pyrolysis, *Current Applied Physics*, **12**, 56-58(2012).

[24] M.R. Vaezi. SnO2/ZnO double-layer thin films: A novel economical preparation and investigation of sensitivity and stability of double-layer gas sensors, *Materials Chemistry and Physics*,**110**, 89-94(2008).

[25] P. Ravikumar, K. Ravichandran, B. Sakthivel, N. Begum, T. Ravichandran, Fabrication of a novel SnO2:Al/ZnO:F bi-layer for opto-electronic applications, *Journal of Materials Science: Materials in Electronics*, **24**, 4092-4097 (2013).

[26] R.Anandhi, K. Ravichandran, R. Mohan. Conductivity enhancement of ZnO:F thin films by the deposition of SnO2:F over layers for optoelectronic applications, *Materials Science and Engineering B*, **178**, 65-70(2013).

[27] S. Karakaya. Effect of fluorine and boron co-doping on ZnO thin films: structural, luminescence properties and Hall effect measurements. *Journal of Materials Science: Materials in Electronics*, **29**, 4080-4088(2018).

[28] C. Moditswe, C. Muiva, A. Juma. Highly conductive and transparent Ga-doped ZnO thin films deposited by chemical spray pyrolysis, *Optik*, **127**, 8317-8325(2016).

[29] A.H. Yahi, A. Bouzidi, R. Miloua, M. Medles, A. Nakrela, M. Khadraoui. The relationship between processing and structural, optical, electrical properties of spray pyrolysed SnO2 thin films prepared for different deposition times, *Optik*, **196** (2019).

[30] A. Ahmed, A. Omar.M. El, A.M. Nawar, S. El-Gazzar ,FaridEl-Tantawy , F.Yakuphanoglu. Semiconducting properties of Al doped ZnO thin films, *Spectrochimica Acta Part A: Molecular and Biomolecular Spectroscopy*, **131**, 512-517(2014).

[31] M. Marikkannan, A. Dinesh, J. Mayandi, V. Vishnukanthan, J.M. Pearce. Properties of Al-doped zinc oxide and In-doped zinc oxide bilayer transparent conducting oxides for solar cell applications, *Materials Letters*, **222**, 50-53(2018).

[32] M.N. Amroun, M. Khadraoui, R. Miloua, Z. Kebbab, K. Sahraoui, Investigation on the structural, optical

and electrical properties of mixed SnS2—CdS thin films, *Optik*, **131**, 152-164(2017).

[33] K. Ravichandran, R. Anandhi1, B. Sakthive, K. Swaminathan, P. Ravikumar, N. Jabena Begum, S. Snega. Thickness Dependence of FTO Over-Layer on Properties of FTO/FZO Bilayer, *Materials and Manufacturing Processes*, **28**, 1322-1326(2013).

[34] W. Szu, T. Lin, S. Jian, J. Juang, S. Jason, T. Jiun. Effects of post-annealing on the structural and nanomechanical properties of Ga-doped ZnO thin films deposited on glass substrate by rf-magnetron sputtering, *Applied Surface Science*, **258**, 1261-1266 (2011).

[35] N. Sadananda, V. Kasturi, G.K. Shivakumar, Effect of annealing on the properties of Bi dopedZnO thin films grown by spray pyrolysis technique, *Superlattices and Microstructures*, **75**, 303-310(2014).

[36] T. Chien, H. Cheng, Y. Tung, W. Tuan, C. Lin. Effect of Sn-doped on microstructural and optical properties of ZnO thin films deposited by sol–gel method, *Thin Solid Films*, **517**, 1032-1036(2008).

[37] R. Mimouni, O. Kamoun, A. Yumak, A. Mhamdi, K. Boubaker, P. Petkova, M. Amlouk. Effect of Mn content on structural, optical, opto-thermal and electrical properties of ZnO:Mn sprayed thin films compounds, *Journal of Alloys and Compounds*, **645**, 100-111(2015).

[38] V. Bilgin, E. Sarica, B. Demirselcuk, S. Turkyilmaz. Iron doped ZnO thin films deposited by ultrasonic spray pyrolysis: structural, morphological, optical, electrical and magnetic investigations. *Journal of Materials Science: Materials in Electronics*, **29**, 17542-17551(2018).

[39] J. Lee, B. Yeo, B. Park, Effects of the annealing treatment on electrical and optical properties of ZnO transparent conduction films by ultrasonic spraying pyrolysis, *Thin Solid Films*, **457**, 333-337(2004).

[40] Y. Aoun, B. Benhaoua, B. Gasmi. Effect of annealing temperature on structural, optical and electrical properties of Zinc oxide (ZnO) thin films deposited by spray pyrolysis technique, *Optik*, **126**, 5407-5411(2015).

[41] A. Davoodia, M. Tajally, O. Mirzaee, A. Eshaghi. The effects of Ti concentration on the structure, optical, and electricalproperties of Al and Ti co-doped ZnO thin films, *Optik*, **127**, 4645-4649(2016).

[42] S. Jafari, M. Hassan, F. Zahedi. Optical and Electrical Properties of a Metal-Semiconductor-Metal Material Based on Al-Doped ZnO Films for Use as UV Photodetectors, *Journal of the Korean Physical Society*, **74**, 1011-1018(2019).

[43] N. Rajeswari, A. Chandra.Burstein–Moss shift and room temperature near-band-edge luminescence in lithium-doped zinc oxide, *Applied Physics A*, **103**, 33-42(2011).

[44] S. Benramache, B. Benhaoua. Influence of annealing temperature on structural and optical properties of ZnO: In thin films prepared by ultrasonic spray technique, *Superlattices and Microstructures*, **52**, 1062-1070(2012).

[45] R. Miloua, Z. Kebbab, B. Noureddine, Pareto-optimal transparent conductive oxides, *RSC Advances*, **2**, 3210-3213(2012).

[46] G. Prakash, A. Khare. Structural and linear and nonlinear optical properties of Zn1-xAlxO ($0 \leq x \leq 0.10$) thin films fabricated via pulsed laser deposition technique, *Optical Materials*, **6**, 2063-2080(2016).

[47] M. Vasanthi, K. Ravichandran, N. Jabena, G. Muruganantham, S. Snega, A. Panneerselvam, P. Kavitha. Influence of Sn doping level on antibacterial activity and certain physical properties of ZnO films deposited using a simplified spray pyrolysis technique, *Superlattices and Microstructures*, **55**, 180-190(2013).

[48] S.S. Shinde, A.P. Korade, C.H. Bhosale, K.Y. Rajpure. Influence of tin doping onto structural, morphological, optoelectronic and impedance properties of sprayed ZnO thin films, *Journal of Alloys and Compounds*, **551**, 688-693(2013).

[49] H. Belkhalfa, H. Ayed, A. Hafdallah, M.S. Aida, R.Tala. Characterization and studying of ZnO thin films deposited by spray pyrolysis: Effect of annealing temperature, Optik., **127**, 2336-2340(2016).

[50] H. Asl, M. Seyed. High quality spray deposited fluorinedoped tin oxide: effect of film thickness on structural, morphological, electrical, and optical properties, *Applied Physics A*, **4**,125-689(2019).

[51] S. Vrushali, K. Sonawane, M. Bhole, S. Patil. Electrical and optical properties of transparent conducting tin doped ZnO thin films, *Journal of Materials Science: Materials in Electronics*, **23**, 451-456(2012).

[52] M. Islam, M. Rahman, M. Khan, M. Halim, M. Sattar, A. Hakim. Spray pyrolized Ag–N co-doped p-type ZnO thin films' preparation and study of their structural, surface morphology and opto-electrical properties, *Thin Solid Films*, **534**, 137-143(2013).

[53] G. Kenanakis, N. Katsarakis, E. Koudoumas, Influence of precursor type, deposition time and doping concentration on the morphological, electrical and optical properties of ZnO and ZnO:Al thin films grown by ultrasonic spray pyrolysis, *Thin Solid Films*, **555**, 62-67(2014).

[54] C. Goebbert, R. Nonninger, M.A. Aegerter, H. Schmidt, Wet chemical deposition of ATO and ITO coatings using crystalline nanoparticles redispersable in solutions, *Thin Solid Films*, **351**, 79-84(1999).

[55] K. Kumara, S. Valanarasua, S. Rex. Preparation and Characterization of Sol–Gel Dip Coated Al: ZnO (AZO) Thin Film for Opto-Electronic Application, *Semiconductors*, **53**, 447-451(2019).